5.2.1.1.3 Test Under Maximum Water Gas Shift Conditions

Highly dispersed ruthenium Catalyst 4966-72 was retested in Run 25 at twice the space velocity relative to Run 21 (140 GHSV). Also a H_2:CO feed ratio = 2.0 was used (Figures 5-122 through 5-126).

The water yield defined as the conversion of CO in the Fischer-Tropsch reaction minus the conversion of CO in the water gas shift reaction was much lower in Run 25 relative to Run 21 (Figure 5-126). Nevertheless, STEM examination indicated that most of the alumina particles contained agglomerated ruthenium in the size range 4 to 50 nm like in Run 21 (Figures 5-127 and 5-128).

These results indicate that the magnitude of steam partial pressure did not have major effect on ruthenium migration and agglomeration.

Figure 5-122. Highly Dispersed Ruthenium Catalyst 4966-72 Conversions in Run 25 (H_2:CO Feed Ratio = 2.0, 208°C at Inlet, 35 atm)

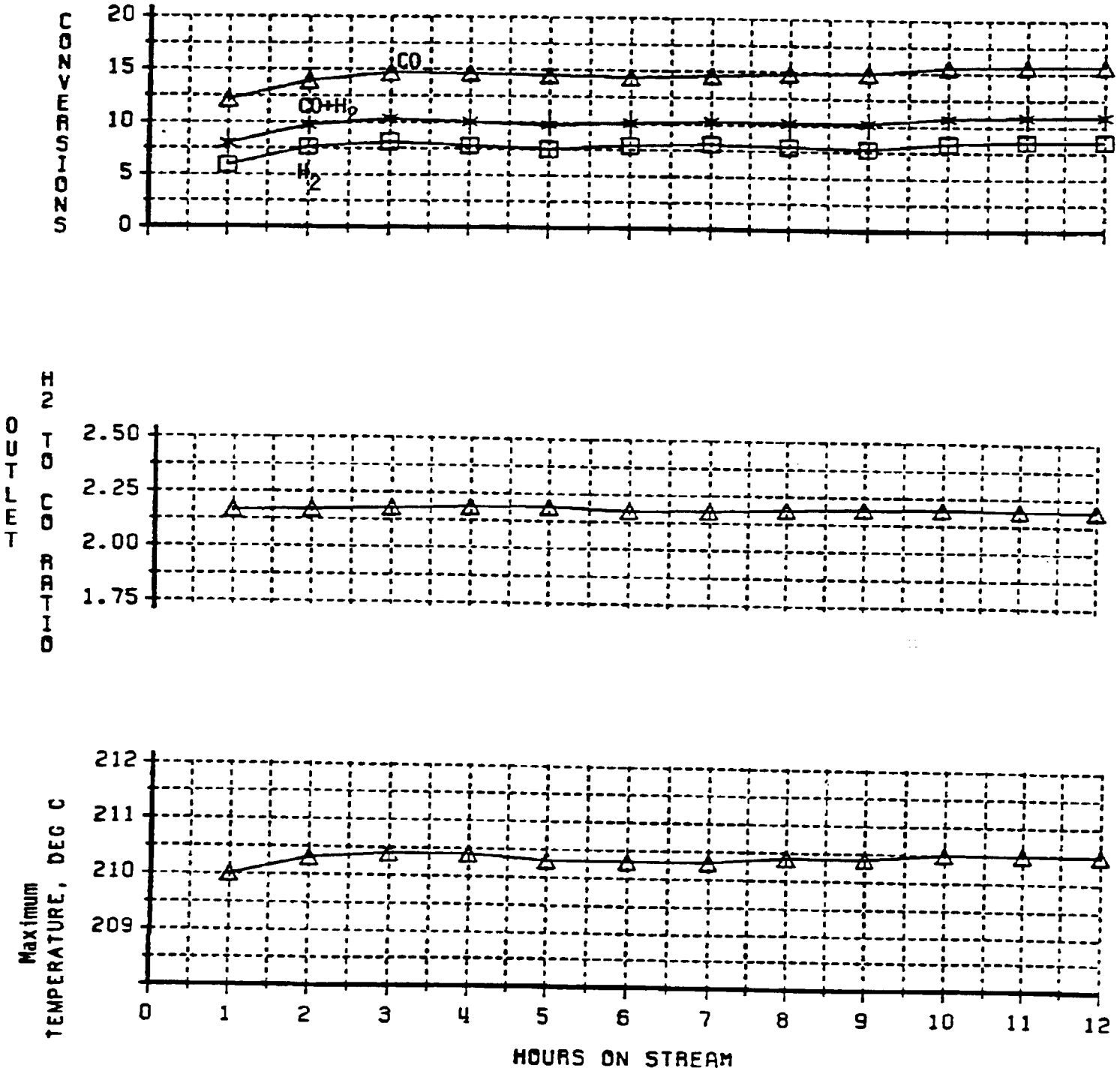

Figure 5-123. Highly Dispersed Ruthenium Catalyst 4966-72 Water Gas Shift Activity in Run 25 (H_2:CO Feed Ratio = 2.0, 208°C at Inlet, 35 atm)

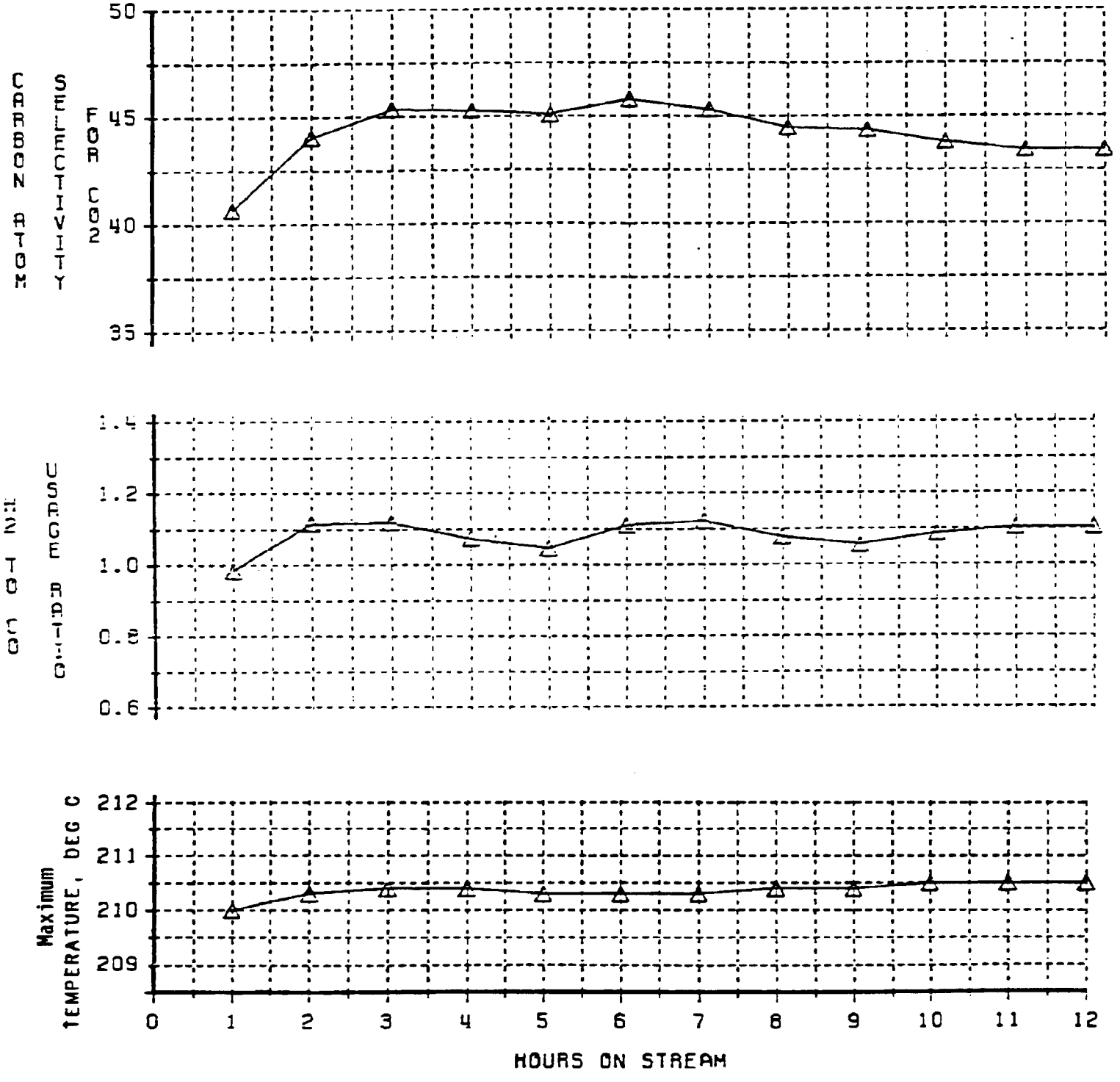

Figure 5-124. Highly Dispersed Ruthenium Catalyst 4966-72 C_1 and C_2 Selectivities in Run 25 (H_2:CO Feed Ratio = 2.0, 208°C at Inlet, 35 atm)

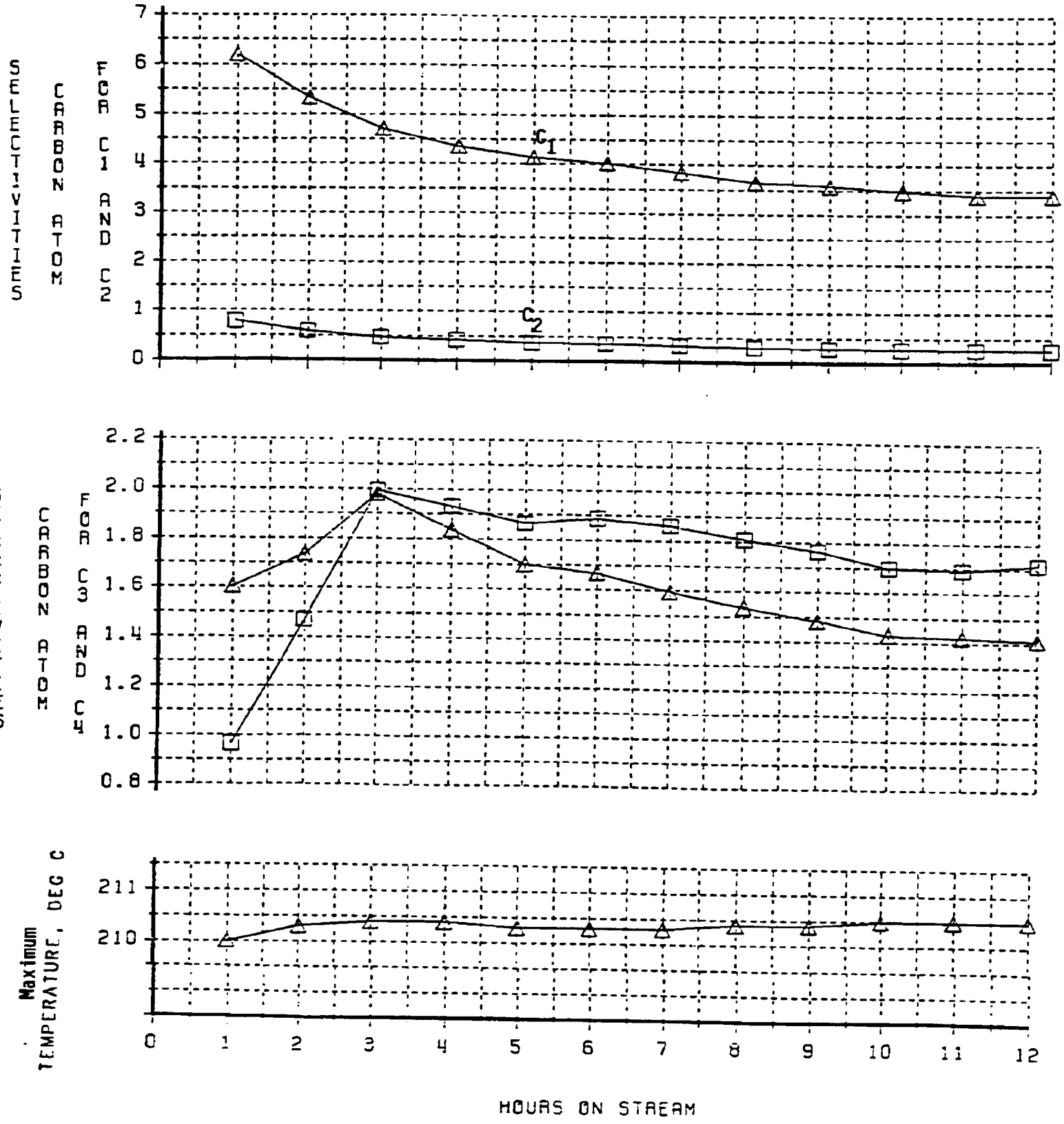

Figure 5-125. Highly Dispersed Ruthenium Catalyst 4966-72 Olefin to Paraffin Ratios in Run 25 (H_2:CO Feed Ratio = 2.0, 208°C at Inlet, 35 atm)

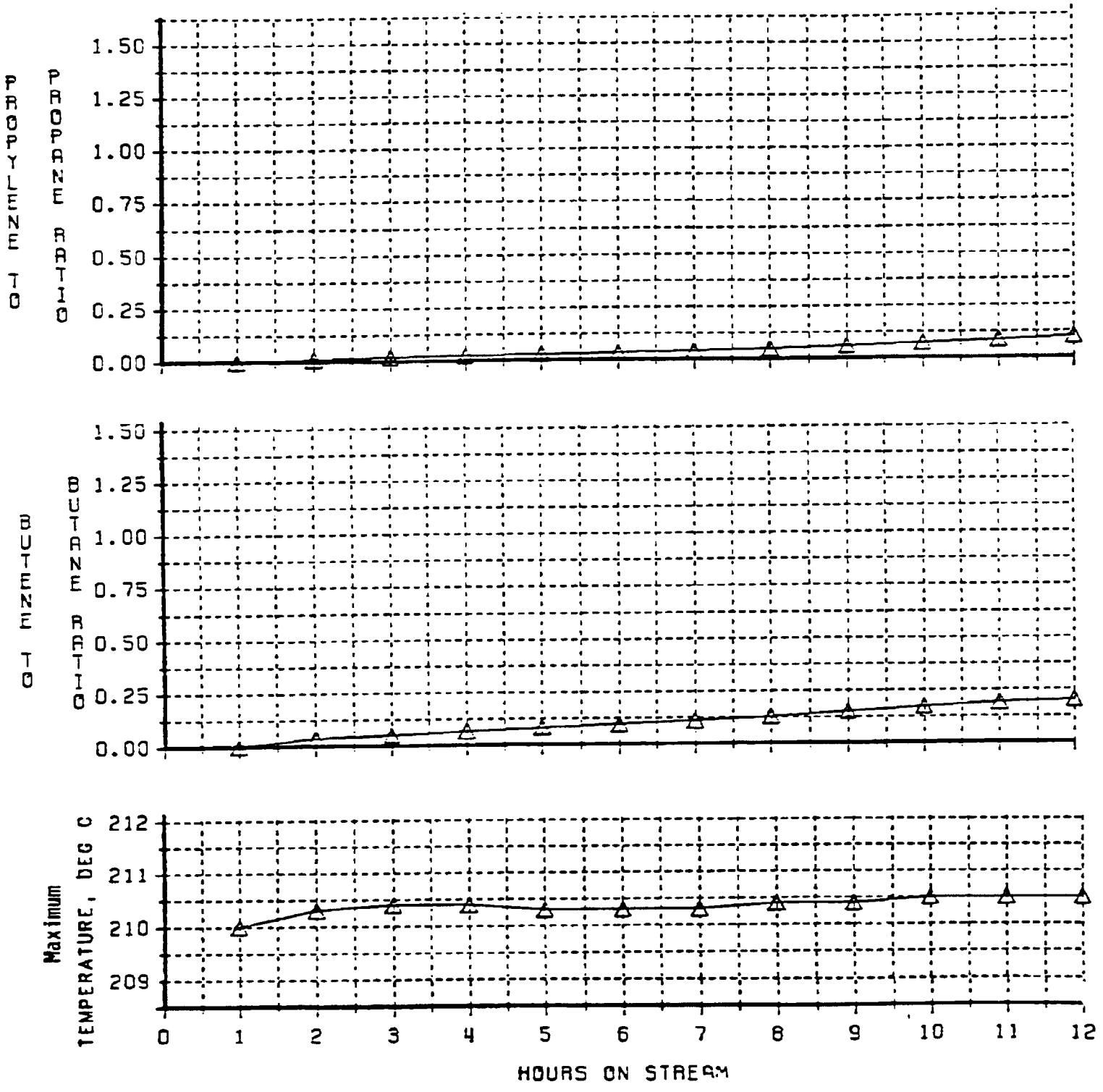

Figure 5-126. Comparison of Water Yields with Highly Dispersed Ruthenium Catalyst 4966-72 in Runs 21 and 25

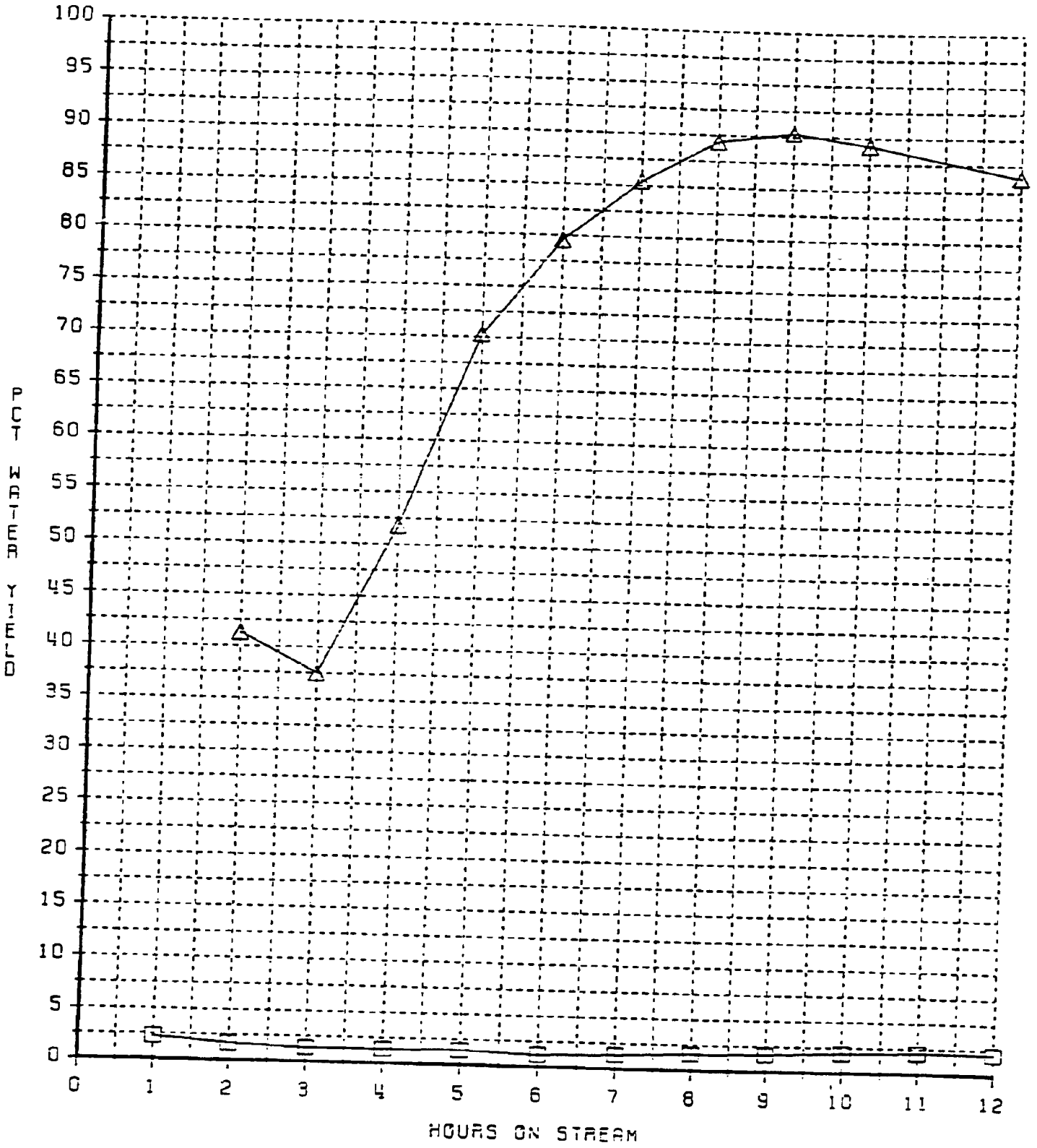

Ruthenium Metal Agglomeration During Fischer-Tropsch Synthesis with Well-Dispersed Ru/γ-Al_2O_3 Catalyst

(STEM Micrographs)

Figure 5-127

FRESH
(0.8 NM Ru by EXAFS)

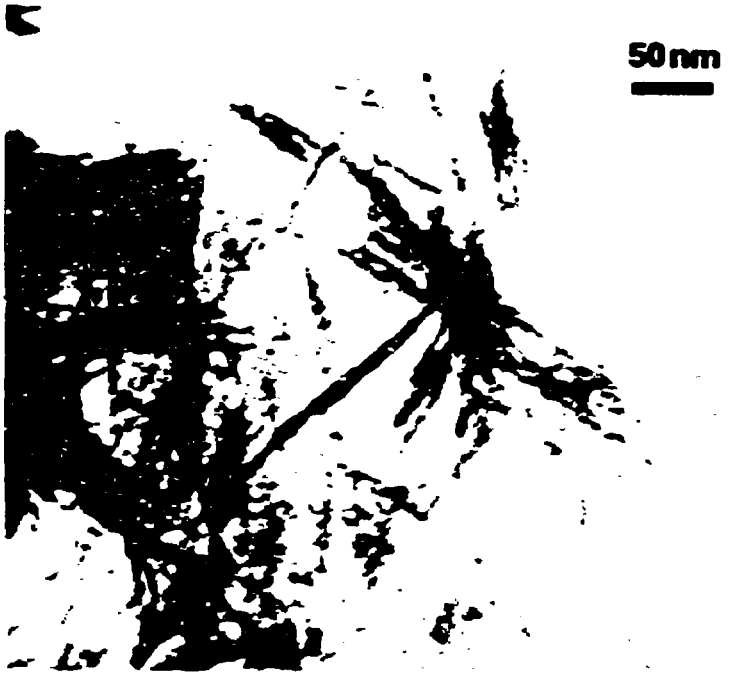

Figure 5-128

USED

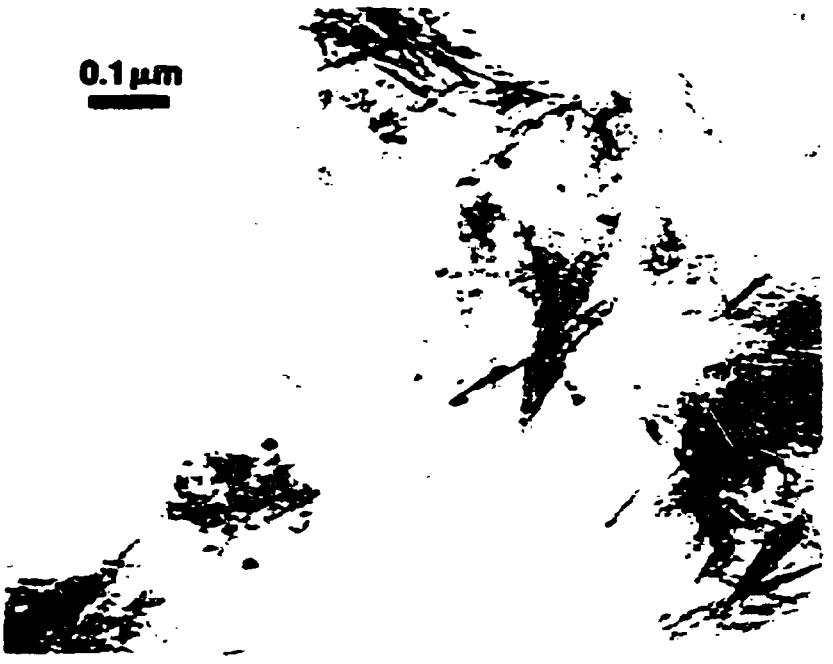

5.2.1.1.4 Test at H_2:CO Feed Ratio = 2.0, 225°C at Inlet and 35 atm

Catalyst 4966-72 with highly dispersed ruthenium was tested in Run 32 at 225°C, 35 atm with 2.0 H_2:1 CO feed gas at space velocities in the range 100-425 GHSV in order to determine the effect of conversion level on light ends selectivity and on olefin:paraffin ratio (Figures 5-129 through 5-132).

Initially at 425 GHSV, the CO+H_2 conversion was 14%. After testing at lower space velocities, the space velocity was brought back to 425 GHSV at 34 hours on stream. The CO+H_2 conversion was about 10% by the end of the test, which indicates that there was some loss in the hydrocarbon synthesis activity of the catalyst. The decline in water gas shift activity was apparently much more rapid, like in other tests with highly dispersed ruthenium catalysts. The CO_2 selectivity declined from 36% to 2% and the H_2:CO usage ratio increased from 0.5 to 2.0 by the end of 20 hours.

The selectivity to C_1-C_4 hydrocarbons decreased with an increase in the conversion level (Figures 5-129 and 5-132). The light ends selectivity was much lower at the end of the run relative to the beginning of the run although the conversion levels were not very different. This indicates that light ends selectivity decreased with time on stream.

During the first 7 hours in Run 32, the olefin to paraffin ratio gradually increased although the conversion level, the outlet H_2:CO ratio and the catalyst maximum temperatures did not change (Figure 5-132).

The propylene to propane ratio decreased with decrease of the space velocity to 100 hr^{-1} at 15 hours on stream. The propylene to propane ratio then started to increase after 22 hours although the space velocity was then even lower: 65 hr^{-1}. At the end of the run, the olefin to paraffin ratio was significantly higher than the value at the beginning of the run at the same space velocity.

Figure 5-129a. Highly Dispersed Ruthenium Catalyst 4966-72 Conversions in Run 32 (H_2:CO Feed Ratio = 2.0, 225°C at Inlet, 35 atm)

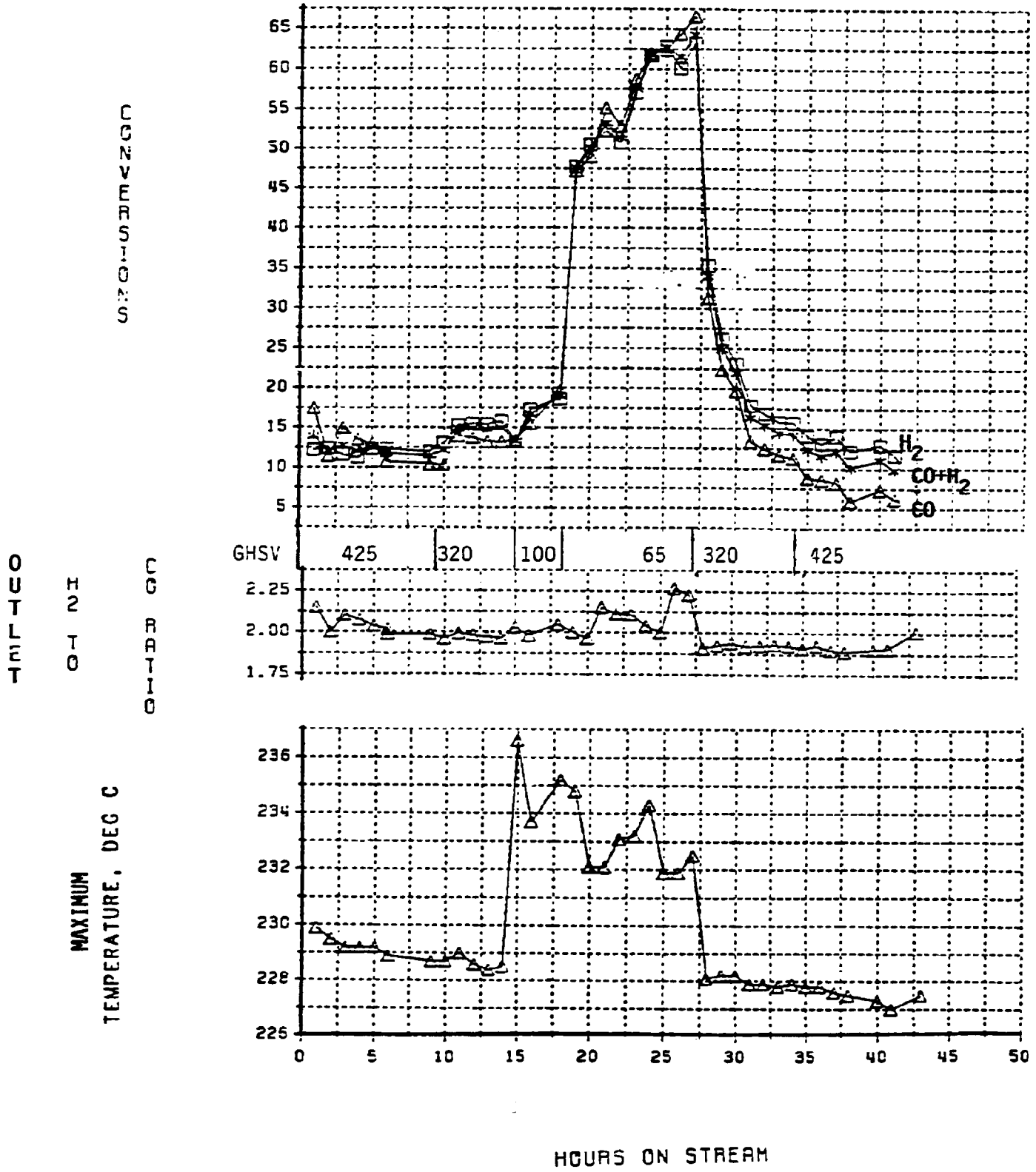

Figure 5-129b. Highly Dispersed Ruthenium Catalyst 4966-72 C_1 and C_2 Selectivities as a Function of Conversion Level in Run 32 (H_2 Feed Ratio = 2.0, 225°C at Inlet, 35 atm)

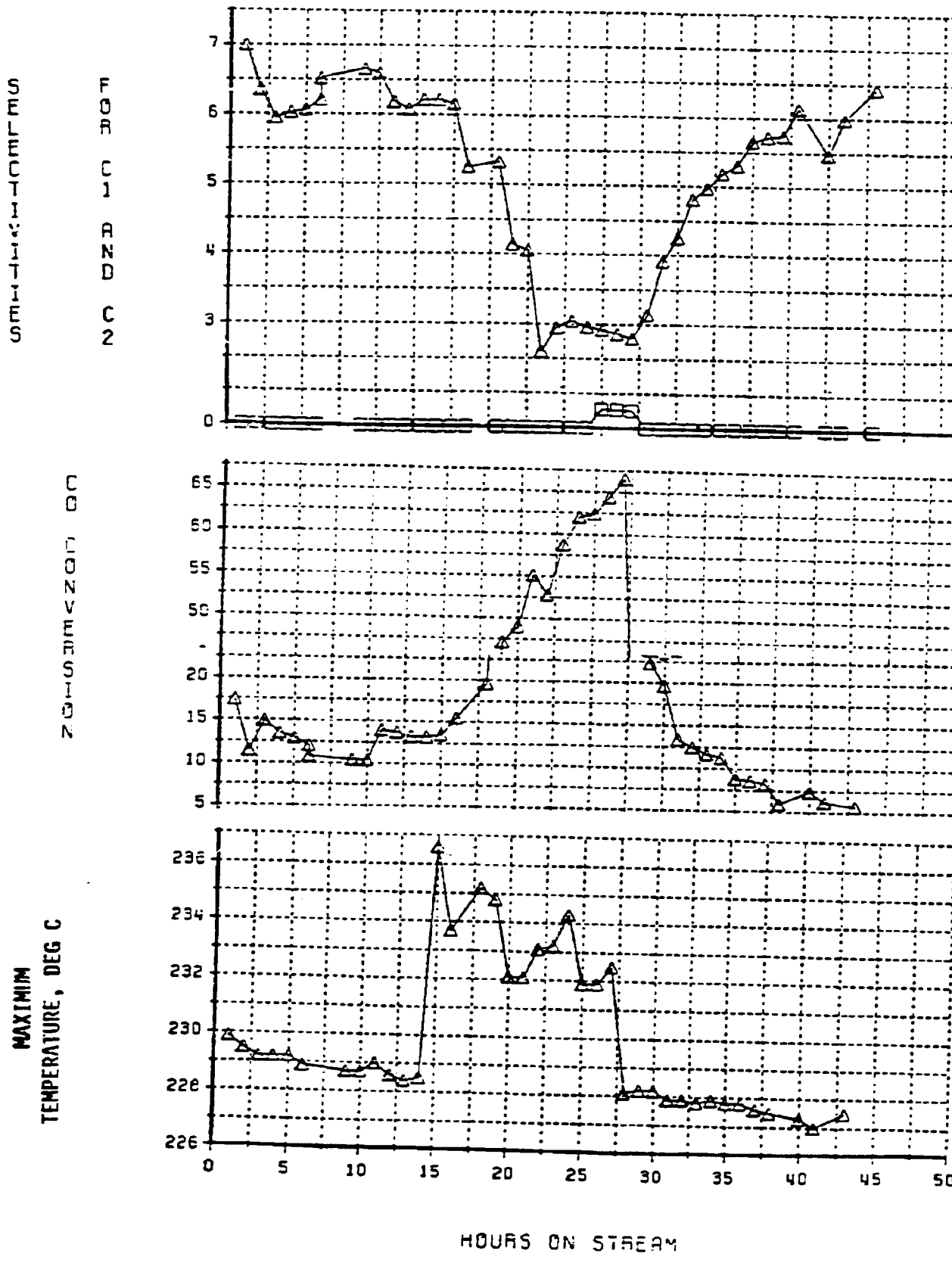

Figure 5-130. Highly Dispersed Ruthenium Catalyst 4966-72 C_3 and C_4 Selectivities as a Function of Conversion Level in Run 32 (H_2:CO Feed Ratio = 2.0, 225°C at Inlet, 35 atm)

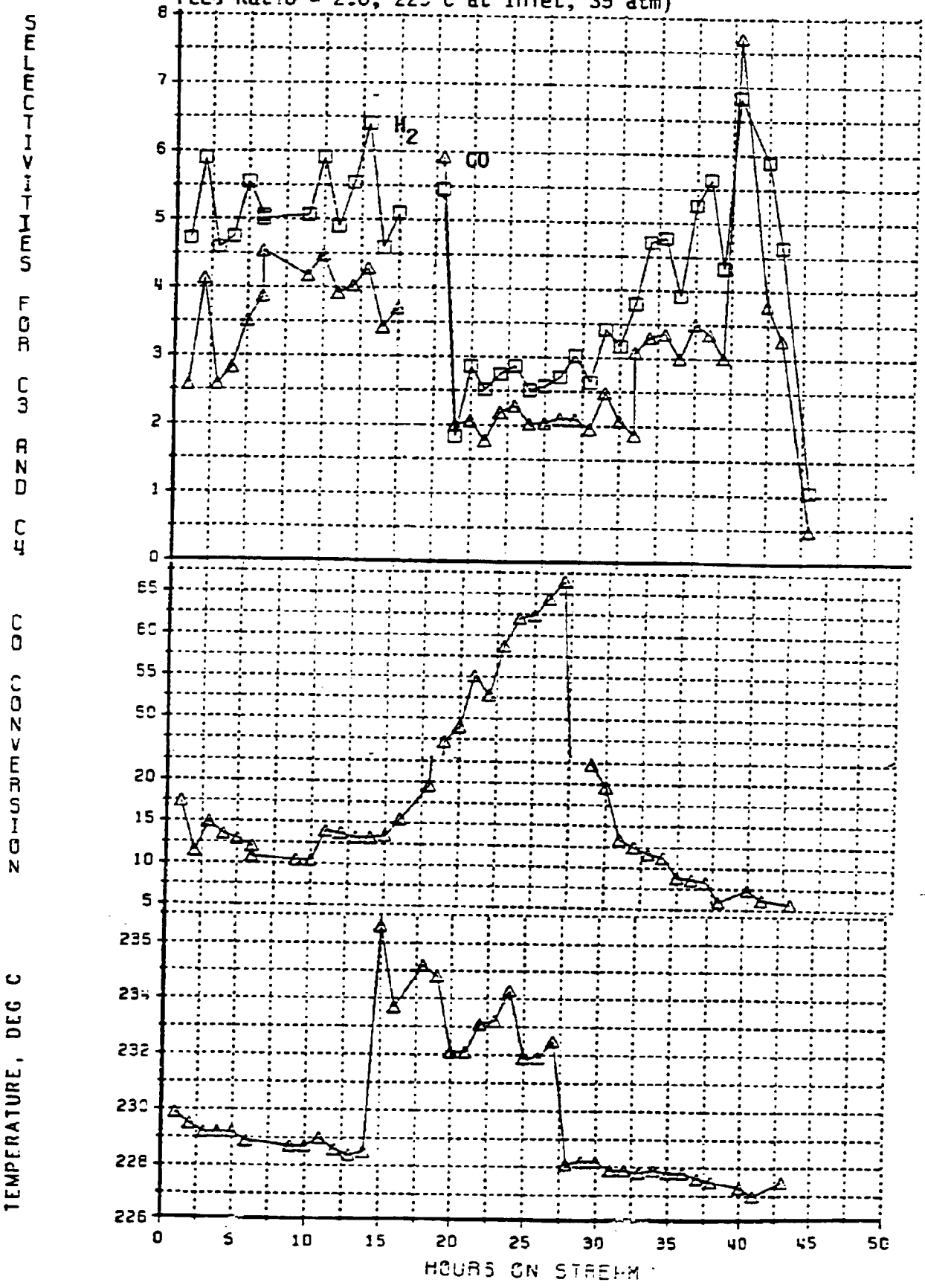

Figure 5-131. Highly Dispersed Ruthenium Catalyst 4966-72 Water Gas Shift Activity as a Function of Conversion Level in Run 32 (H_2:CO Feed Ratio = 2.0, 225°C at Inlet, 35 atm)

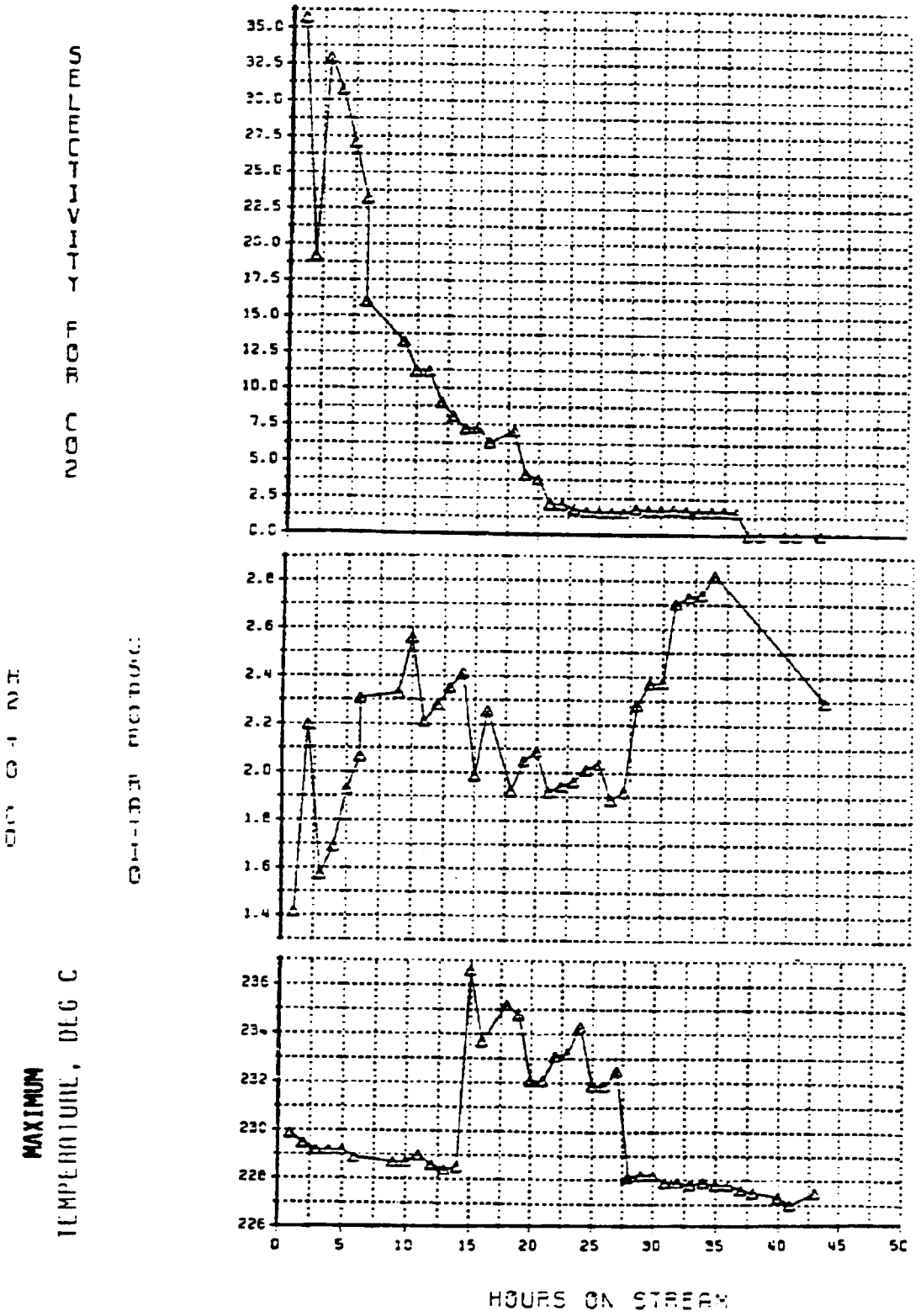

Figure 5-132. Highly Dispersed Ruthenium Catalyst 4966-72 Propylene:Propane Ratio as a Function of Conversion Level in Run 32 (H_2:CO Feed Ratio = 2.0, 225°C at Inlet, 35 atm)

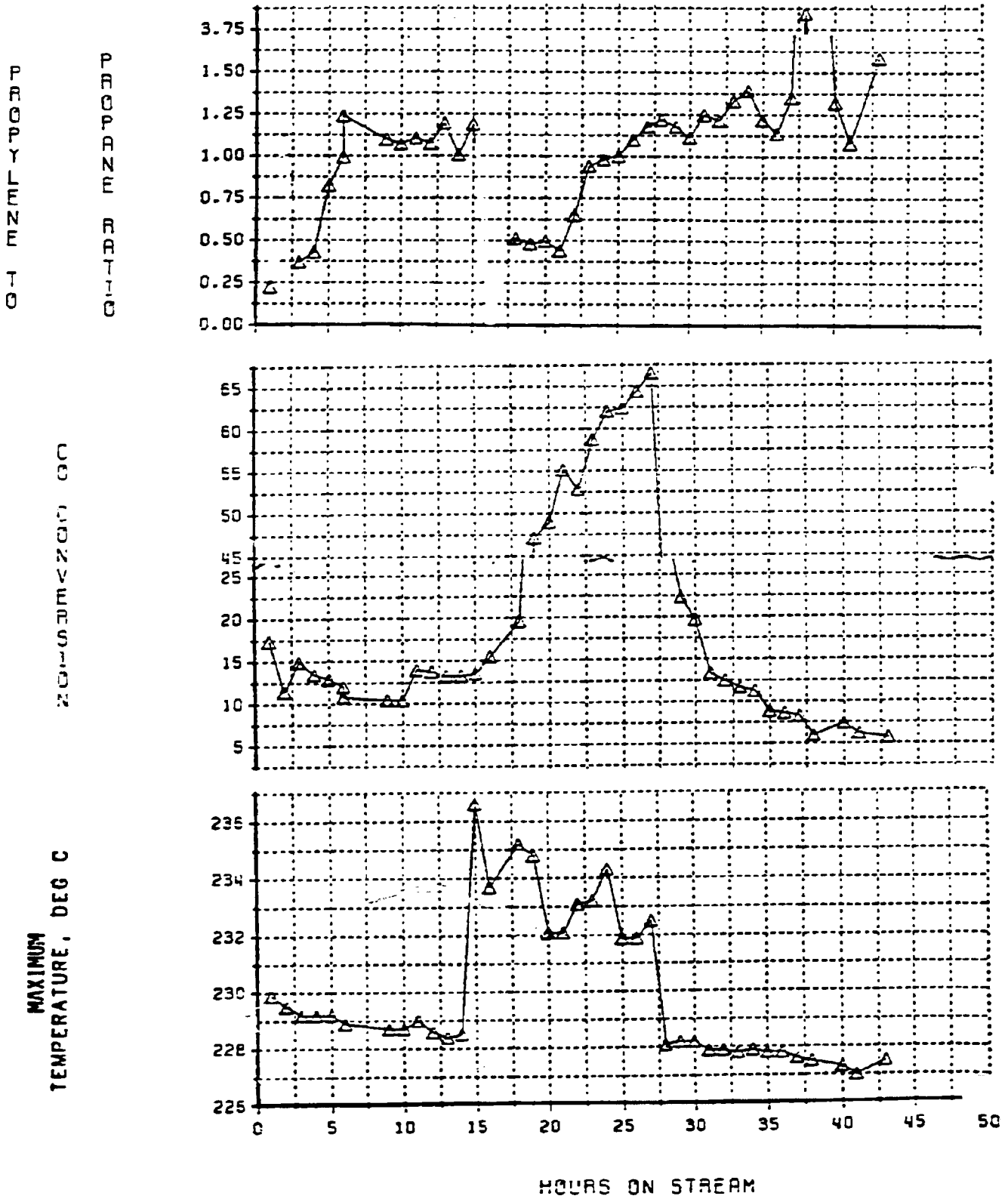

5.2.1.2 Catalysts with ≤2-4 nm Ru Particles with ~1% Ru (by wt.)

Various tests with highly dispersed ruthenium catalysts indicated that ruthenium metal agglomeration via the formation of the volatile ruthenium carbonyl species occurred rapidly during Fischer-Tropsch synthesis. Therefore, it was not possible to determine whether hydrocarbon cutoff occurred with small ruthenium metal particles. Therefore, catalysts with slightly larger (≤2-4 nm) ruthenium metal particles were tested.

5.2.1.2.1 Test at 0.9 H_2:CO Feed Ratio, 208°C at Inlet and 35 atm

Catalyst 4956-101 with ≤2-4 nm ruthenium particles was tested at 208°C inlet temperature, 35 atm, 68 GHSV with a 0.9 H_2:CO feed ratio synthesis gas in Run 17 (Tables 5-24 and 5-25 and Figures 5-133 through 5-140).

The initial CO conversion was 32%, which is higher than that obtained with the highly dispersed ruthenium catalyst tested in Run 16. The CO conversion in Run 17 decreased to 23% by 10 nours on stream (Figure 5-133). Early in the run, the catalyst's water gas shift activity also decreased, as it is apparent from the rapid decline in CO_2 selectivity, from 42% at 7 hours on stream to 8% at 12 hours on stream. This decrease in CO_2 selectivity was accompanied by an increase in the H_2:CO usage ratio from 0.8 to 1.8 (Figure 5-134). The CO conversion gradually decreased to 10% by 80 hours on stream after which the decrease was much slower.

At around 212 hours on stream, a plug quickly developed at the outlet of the Fischer Porter cylinder in the freon-cooled box, apparently resulting in pressures exceeding 8 atm. The cylinder exploded within the box, and therefore the products which were collected during the run in the C_9-C_{12} range were lost (Figure 5-139). The run was terminated after this incident.

The gel permeation chromatography results obtained in Run 17 are described in detail in Figure 5-138. The heavier hydrocarbons collected in the reactor outlet and in the high temperature-high pressure separator showed higher average

Table 5-24. Product Distributions in Run 17

TOTAL PRODUCT DISTRIBUTION	
WEIGHT PCTS WITHOUT ARGON	
HYDROGEN	4.950
CARBON MONOXIDE	89.257
CARBON DIOXIDE	1.050
WATER	0.594
HYDROCARBONS	4.149
OXYGENATES	0.000
HYDROCARBON DISTRIBUTION	
C1	1.090
C2 - C4	1.898
C5 - C11	4.926
C12 - C18	2.623
C19 - C25	7.436
C26 PLUS	82.027
C1 - C44	42.162
C45 PLUS	57.838
OXYGENATES DISTRIBUTION	
ALCOHOLS	59.091
ALDEHYDES	40.909
OTHER OXYGENATES	0.000
MOLE PCTS WITHOUT ARGON	
HYDROGEN	42.992
CARBON MONOXIDE	55.793
CARBON DIOXIDE	0.418
WATER	0.577
HYDROCARBONS	0.220
OXYGENATES	0.000
RECOVERIES	
OVERALL	95.040
CARBON	98.467
HYDROGEN	87.288
OXYGEN	91.799
ARGON	101.205
CORRECTED RECOVERIES	
OVERALL	93.908
CARBON	97.294
HYDROGEN	86.249
OXYGEN	90.706

GAS ANALYSIS, WT%	
HYDROGEN	4.9502
CARBON MONOXIDE	89.2567
CARBON DIOXIDE	1.0495
METHANE	0.0452
ETHANE	0.0053
ETHYLENE	0.0099
PROPANE	0.0138
PROPYLENE	0.0136
BUTANE	0.0180
BUTENE	0.0179
AQUEOUS ANALYSIS, WT%	
WATER	0.5941
ALCOHOLS	
C1	0.0001
C2	0.0001
C3	0.0000
C4	0.0000
C5	0.0000
C6	0.0001
C7	0.0000
C8	0.0000
C9	0.0000
C10	0.0000
ALDEHYDES	
C1	0.0000
C2	0.0000
C3	0.0000
C4	0.0001
C5	0.0001
C6	0.0000
C7	0.0000
C8	0.0000
C9	0.0000
C10	0.0000
OTHER OXYGENATES	
C1	0.0000
C2	0.0000
C3	0.0000
C4	0.0000
C5	0.0000
C6	0.0000
C7	0.0000
C8	0.0000
C9	0.0000
C10	0.0000

Table 5-25. Hydrocarbon Distributions in Run 17

C1	1.0901	C51	1.1289	C101	0.3905	C151	0.0933	C201	0.0310
C2	0.3670	C52	1.1112	C102	0.3791	C152	0.0911	C202	0.0305
C3	0.6596	C53	1.0936	C103	0.3679	C153	0.0890	C203	0.0299
C4	0.8711	C54	1.0749	C104	0.3570	C154	0.0869	C204	0.0294
C5	1.0189	C55	1.0572	C105	0.3463	C155	0.0849	C205	0.0289
C6	0.5316	C56	1.0344	C106	0.3359	C156	0.0830	C206	0.0284
C7	0.8082	C57	1.0166	C107	0.3125	C157	0.0811	C207	0.0278
C8	1.0456	C58	0.9987	C108	0.3028	C158	0.0794	C208	0.0273
C9	1.2822	C59	0.9808	C109	0.2934	C159	0.0776	C209	0.0268
C10	0.1966	C60	0.9636	C110	0.2843	C160	0.0759	C210	0.0263
C11	0.0432	C61	0.9460	C111	0.2754	C161	0.0743	C211	0.0259
C12	0.0574	C62	0.9286	C112	0.2668	C162	0.0727	C212	0.0254
C13	0.1541	C63	0.9188	C113	0.2585	C163	0.0712	C213	0.0249
C14	0.2631	C64	0.9020	C114	0.2505	C164	0.0697	C214	0.0244
C15	0.5844	C65	0.8854	C115	0.2427	C165	0.0683	C215	0.0240
C16	0.4304	C66	0.8691	C116	0.2352	C166	0.0669	C216	0.0235
C17	0.5148	C67	0.8528	C117	0.2279	C167	0.0655	C217	0.0231
C18	0.6184	C68	0.8369	C118	0.2208	C168	0.0642	C218	0.0226
C19	0.8742	C69	0.8212	C119	0.2140	C169	0.0616	C219	0.0222
C20	0.8692	C70	0.8056	C120	0.2074	C170	0.0604	C220	0.0217
C21	0.9518	C71	0.8110	C121	0.2010	C171	0.0591	C221	0.0213
C22	1.0581	C72	0.7956	C122	0.1948	C172	0.0579	C222	0.0209
C23	1.1688	C73	0.7803	C123	0.1888	C173	0.0568	C223	0.0205
C24	1.2173	C74	0.7652	C124	0.1905	C174	0.0556	C224	0.0200
C25	1.2970	C75	0.7500	C125	0.1849	C175	0.0545	C225	0.0196
C26	1.3280	C76	0.7349	C126	0.1795	C176	0.0534	C226	0.0192
C27	1.3541	C77	0.7198	C127	0.1743	C177	0.0523	C227	0.0188
C28	1.3284	C78	0.7049	C128	0.1692	C178	0.0513	C228	0.0184
C29	1.3807	C79	0.6900	C129	0.1644	C179	0.0503	C229	0.0180
C30	1.3798	C80	0.6753	C130	0.1697	C180	0.0493	C230	0.0176
C31	1.3667	C81	0.6505	C131	0.1551	C181	0.0483	C231	0.0172
C32	1.3568	C82	0.6359	C132	0.1507	C182	0.0473	C232	0.0168
C33	1.3354	C83	0.6215	C133	0.1465	C183	0.0464	C233	0.0164
C34	1.3259	C84	0.6071	C134	0.1424	C184	0.0455	C234	0.0161
C35	1.3136	C85	0.5929	C135	0.1385	C185	0.0446	C235	0.0157
C36	1.2941	C86	0.5788	C136	0.1347	C186	0.0437	C236	0.0153
C37	1.2716	C87	0.5648	C137	0.1310	C187	0.0428	C237	0.0070
C38	1.2558	C88	0.5509	C138	0.1275	C188	0.0420	C238	0.0069
C39	1.2249	C89	0.5372	C139	0.1240	C189	0.0411	C239	0.0068
C40	1.1855	C90	0.5235	C140	0.1207	C190	0.0403	C240	0.0067
C41	1.2355	C91	0.5101	C141	0.1176	C191	0.0395	C241	0.0066
C42	1.1202	C92	0.4967	C142	0.1145	C192	0.0387	C242	0.0065
C43	1.0819	C93	0.4899	C143	0.1115	C193	0.0380	C243	0.0064
C44	1.0497	C94	0.4768	C144	0.1110	C194	0.0372	C244	0.0063
C45	1.2001	C95	0.4639	C145	0.1082	C195	0.0364	C245	0.0062
C46	1.1832	C96	0.4512	C146	0.1055	C196	0.0357	C246	0.0062
C47	1.1661	C97	0.4386	C147	0.1029	C197	0.0350	C247	0.0061
C48	1.1487	C98	0.4263	C148	0.1004	C198	0.0342	C248	0.0060
C49	1.1321	C99	0.4141	C149	0.0979	C199	0.0321	C249	0.0059
C50	1.1464	C100	0.4022	C150	0.0956	C200	0.0316	C250	0.0058

Figure 5-133. Catalyst 4956-101 with ≤2-4 nm Ruthenium Particles: Conversions in Run 17 (H_2:CO Feed Ratio = 0.9, 208°C at Inlet, 35 atm)

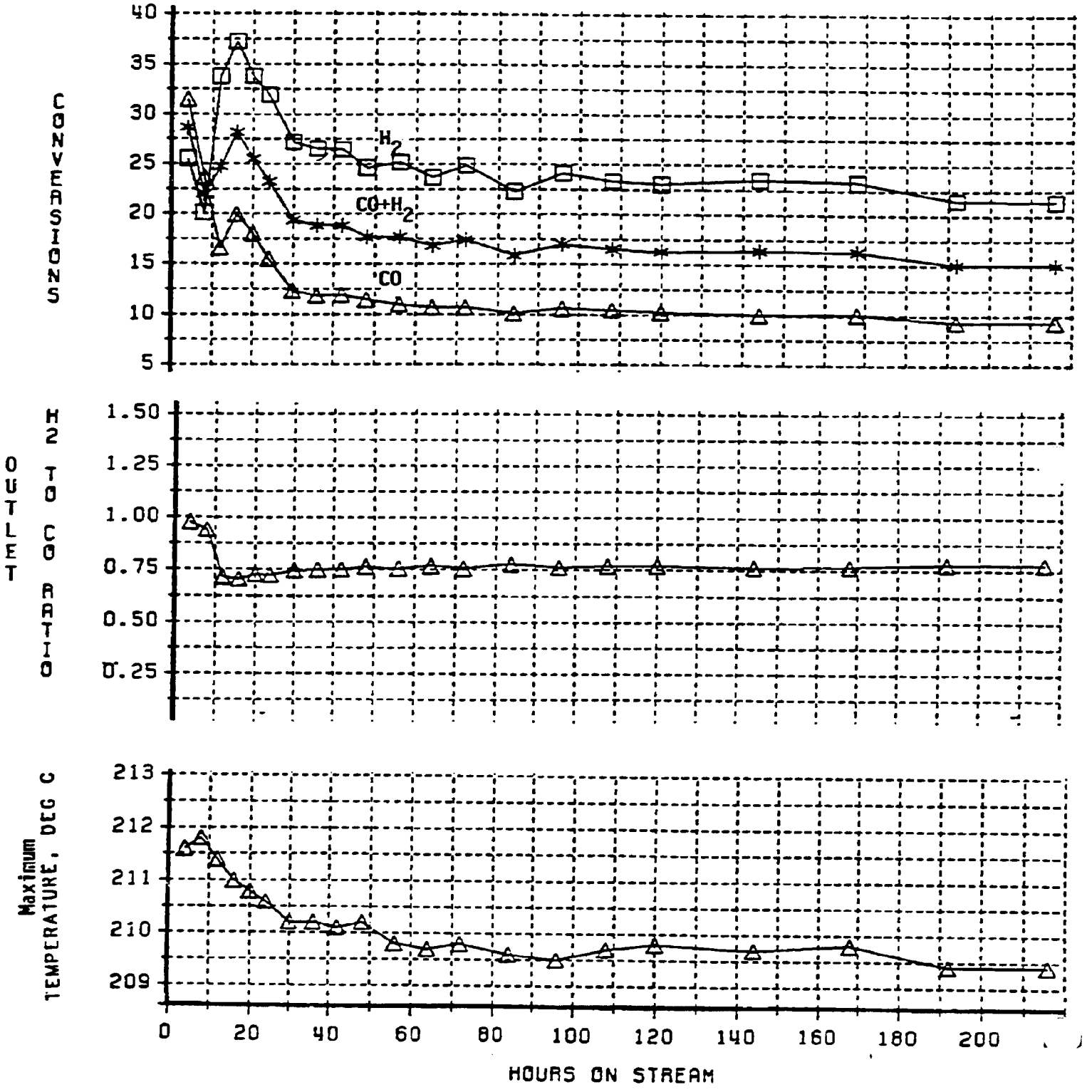

Figure 5-134. Catalyst 4956-101 with <2-4 nm Ruthenium Particles: Water Gas Shift Activity in Run 17 (H_2:CO Feed Ratio = 0.9, 208°C at Inlet, 35 atm)

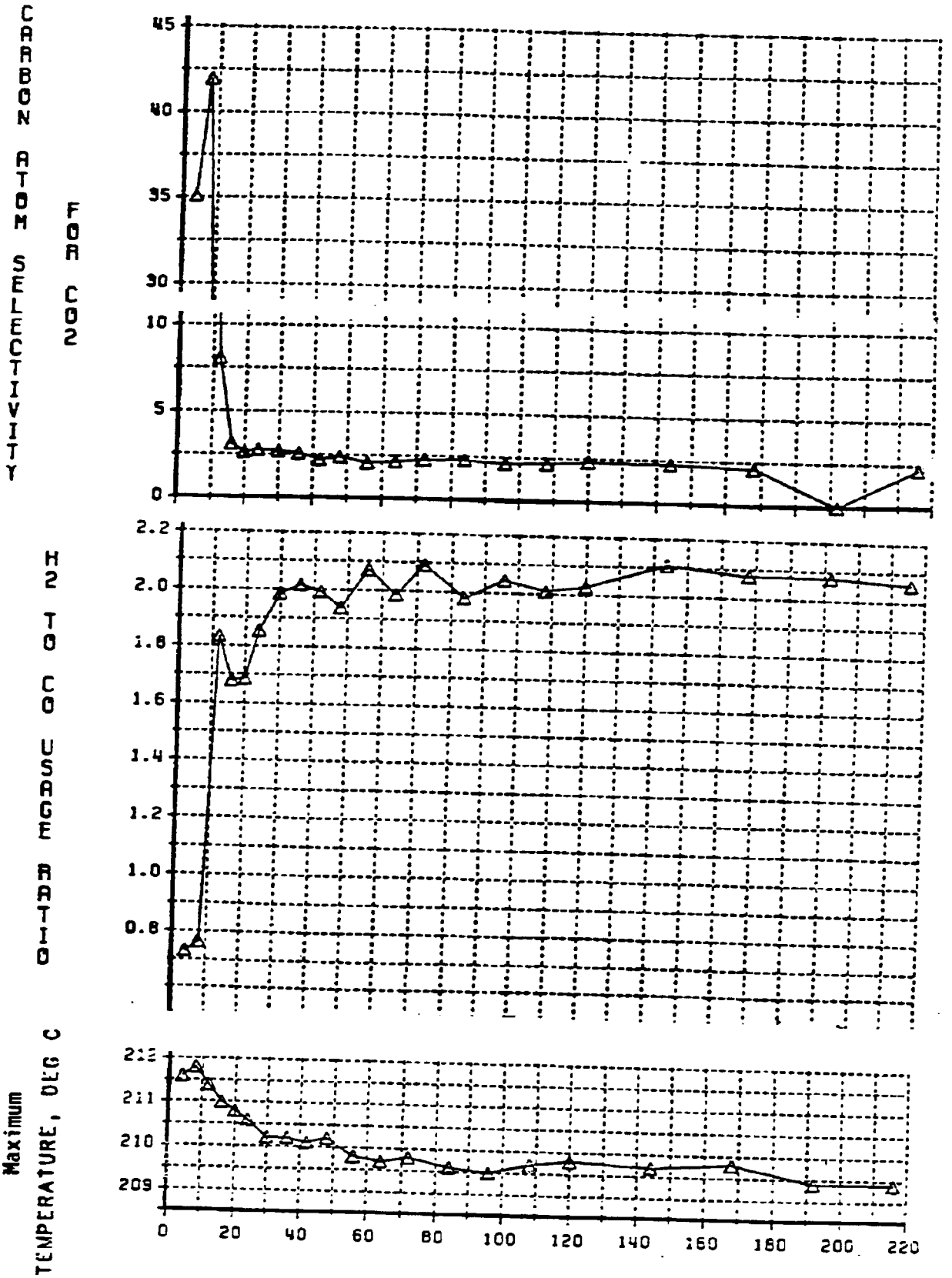

Figure 5-135. Catalyst 4956-101 with <2-4 nm Ruthenium Particles: C_1 and C_2 Selectivities in Run 17 (H_2:CO Feed Ratio = 0.9, 208°C at Inlet, 35 atm)

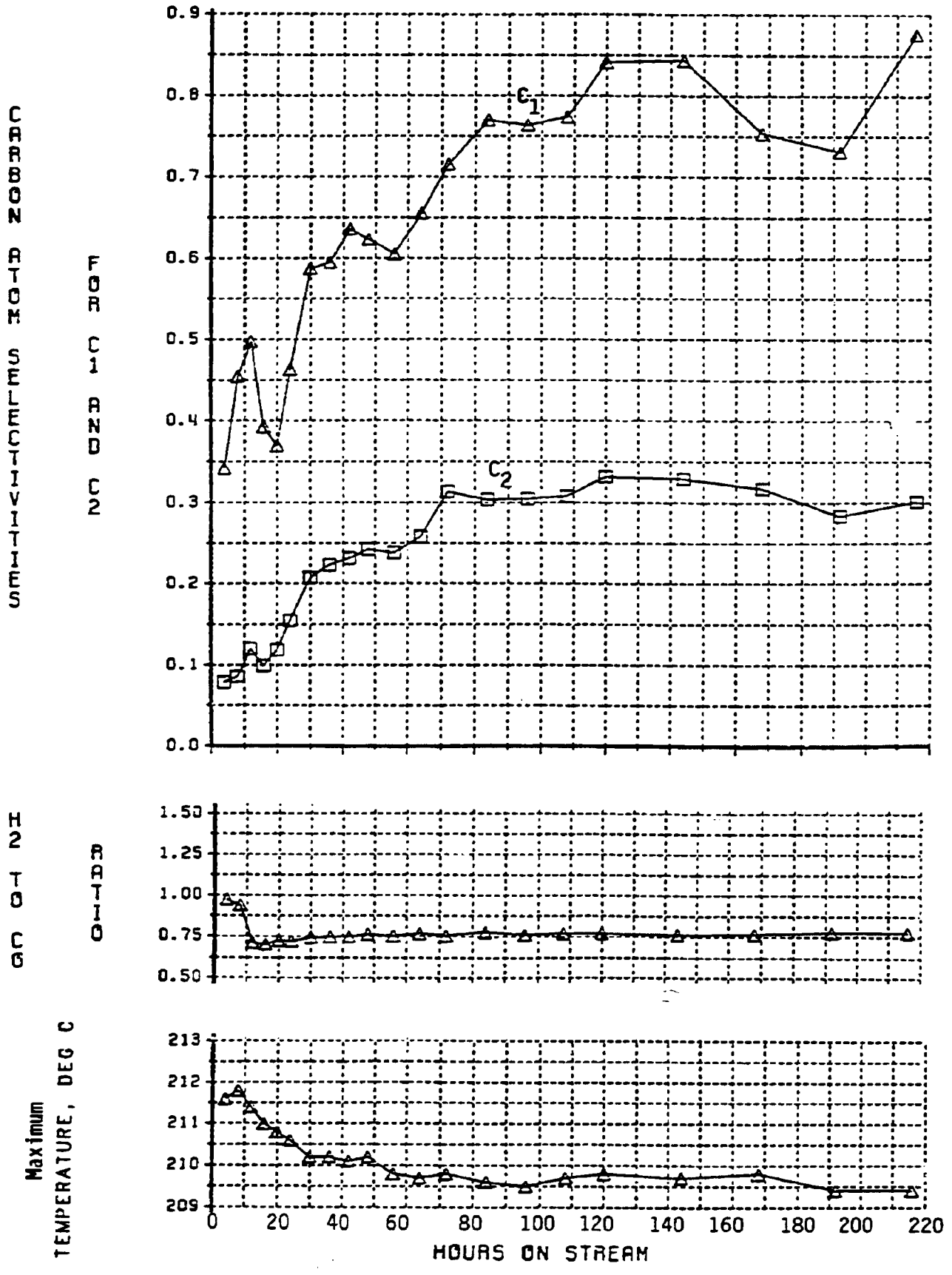

Figure 5-136. Catalyst 4956-101 with <2-4 nm Ruthenium Particles: C_3 and C_4 Selectivities in Run 17 (H_2:CO Feed Ratio = 0.9, 208°C at Inlet, 35 atm)

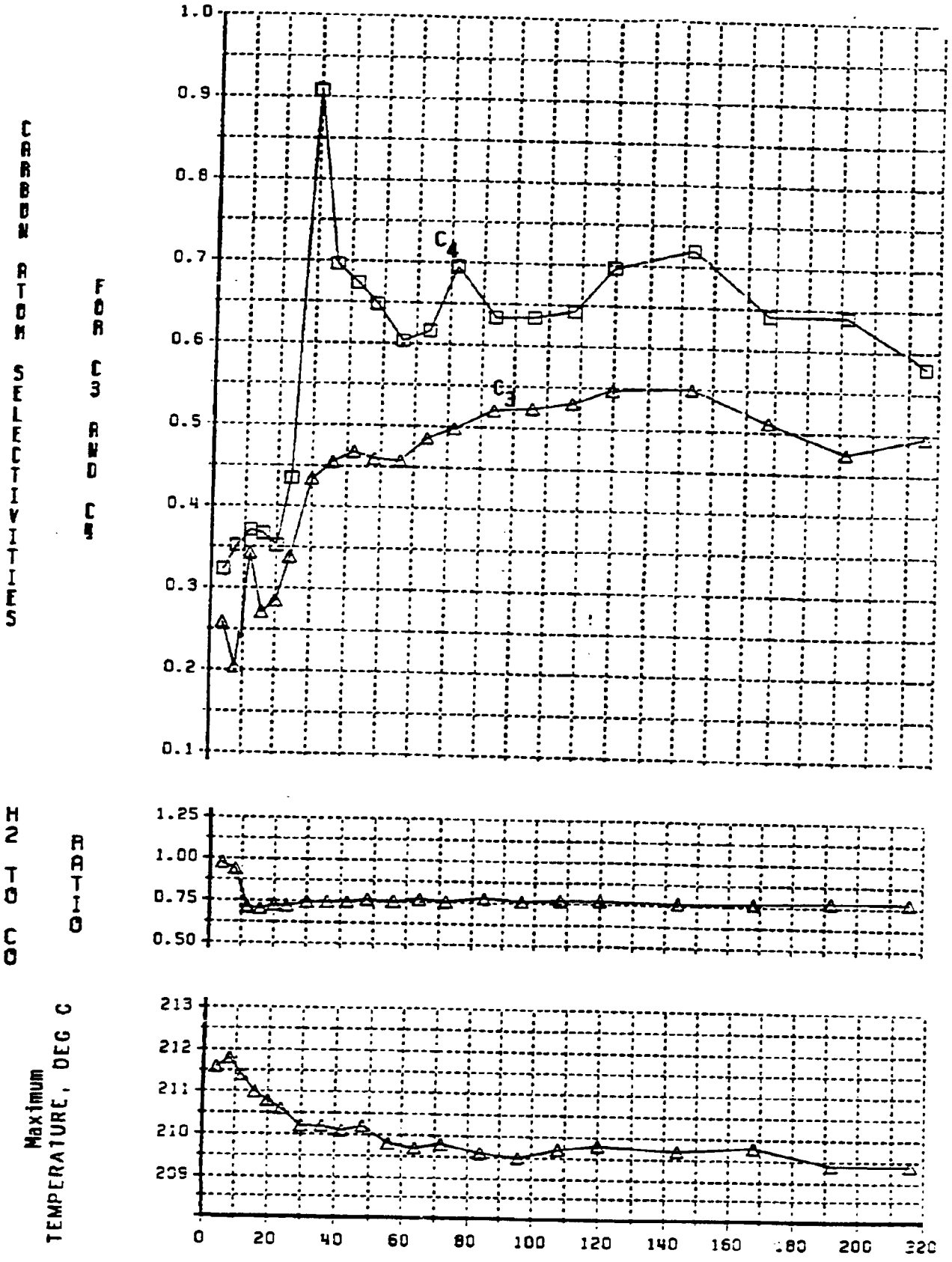

Figure 5-137. Catalyst 4956-101 with ≤2-4 nm Ruthenium Particles: Olefin to Paraffin Ratios in Run 17 (H_2:CO Feed Ratio = 0.9, 208°C at Inlet, 35 atm)

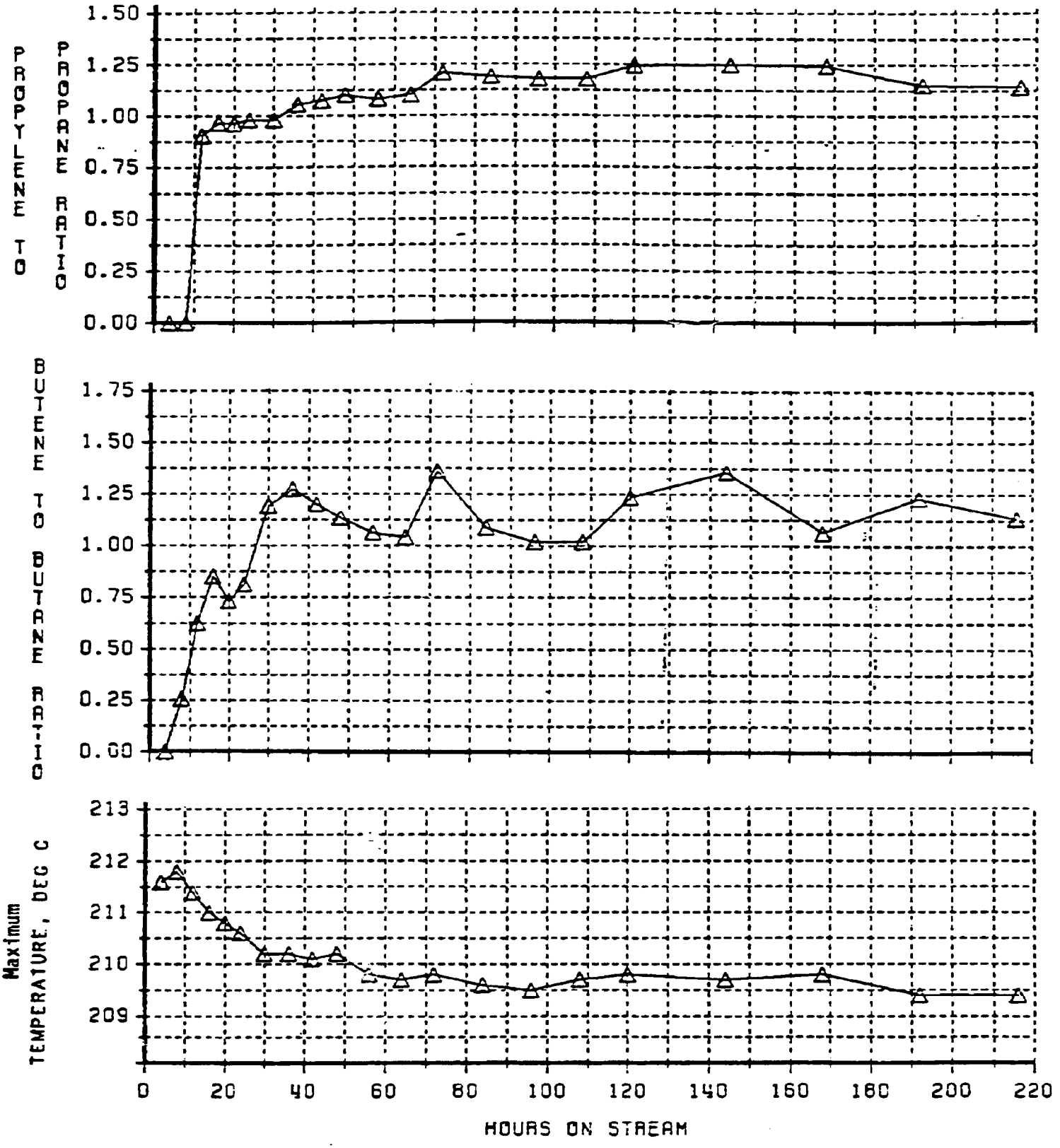

Figure 5-138. Gel Permeation Chromatography Analyses of Products in Run 17

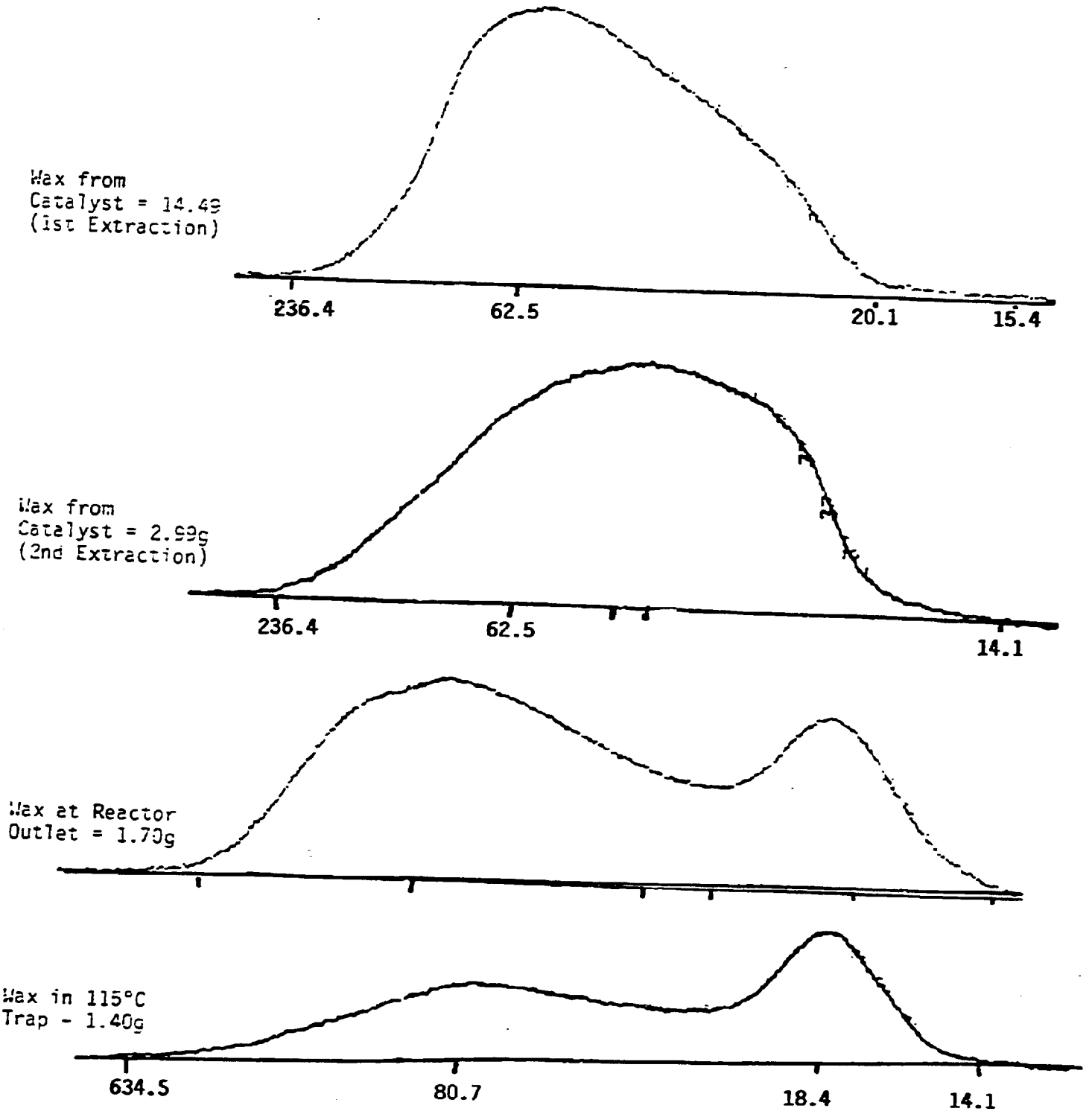

Figure 5-139. Anderson-Schulz-Flory Distribution with Catalyst 4956-101 with ≤2-4 nm Ruthenium Particles in Run 17 (Hydrocarbons + Oxygenates)

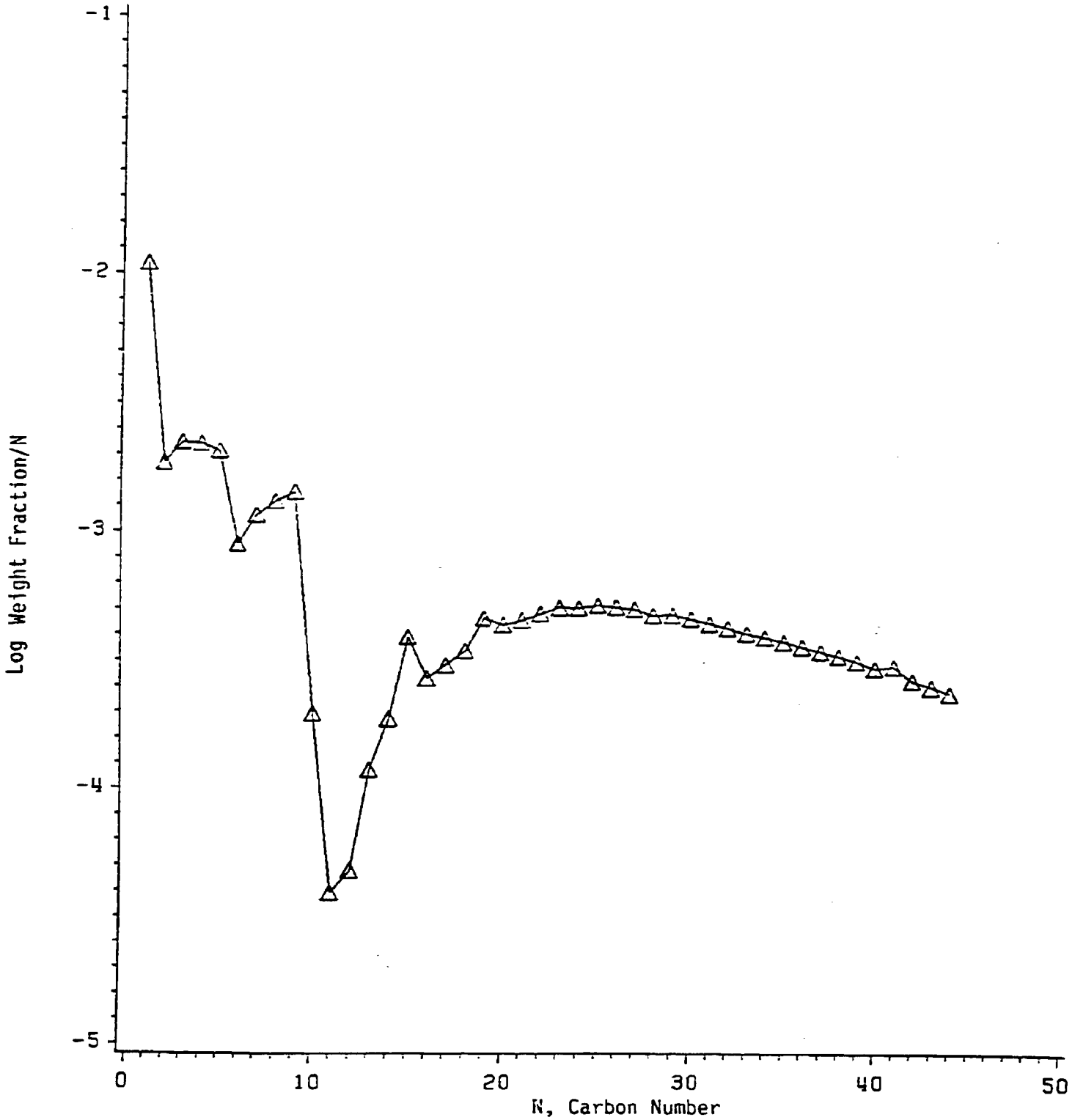

Figure 5-140. Anderson-Schulz-Flory Distribution with Catalyst 4956-101 with ≤2-4 nm Ruthenium Particles in Run 17 (Hydrocarbons Only)